Biosensors and Bioelectronics 31 (2012) 292–298

Contents lists available at SciVerse ScienceDirect

Biosensors and Bioelectronics

journal homepage: www.elsevier.com/locate/bios

Ratiometric fluorescence imaging of dual bio-molecular events in single living cells using a new FRET pair mVenus/mKOκ-based biosensor and a single fluorescent protein biosensor

Ting Su[a,b], Zhihong Zhang[a,b,*], Qingming Luo[a,b]

[a] Britton Chance Center for Biomedical Photonics, Wuhan National Laboratory for Optoelectronics-Huazhong University of Science and Technology, Wuhan 430074, PR China
[b] Key Laboratory of Biomedical Photonics of Ministry of Education, Huazhong University of Science and Technology, Wuhan 430074, PR China

ARTICLE INFO

Article history:
Received 13 September 2011
Received in revised form 14 October 2011
Accepted 18 October 2011
Available online 24 October 2011

Keywords:
Ratiometric fluorescent imaging
Fluorescent protein
Biosensor
mVenus
mKOκ
Grx1-roGFP2

ABSTRACT

Genetically coded fluorescent protein (FP)-based biosensors are powerful tools for the non-invasive tracking of molecular events in living cells. Although a variety of FP biosensors are available, the simultaneous imaging of multiple biosensors (multi-parameter imaging) in single living cells remains a challenge and is far from routinely used to elucidate the intricate networks of molecular events. In this study, we established a novel combination of FP biosensors for dual-parameter ratiometric imaging, consisting of a new fluorescence resonance energy transfer (FRET) pair mVenus (yellow FP)/mKOκ (orange FP)-based (abbreviated as YO) biosensor and a single FP-based biosensor Grx1-roGFP2. Under our imaging condition, $1.4 \pm 0.05\%$ of Grx1-roGFP2 signal contributes to the mVenus channel and $5.2 \pm 0.12\%$ of the mVenus signal contributes to the Grx1-roGFP2 channel. We demonstrate that such low degree of cross-talk causes negligible distortion of the ratiometric signal of the YO-based FRET biosensor and Grx1-roGFP2. By using this dual-parameter ratiometric imaging approach, we achieved simultaneous imaging of Src/Ca^{2+} signaling and glutathione (GSH) redox potential in a single cell, which was previously unattainable. Furthermore, we provided direct evidence that epidermal growth factor (EGF)-induced Src signaling was negatively regulated by H_2O_2 via its effect on GSH-based redox system, demonstrating the power of this dual-parameter imaging approach for elucidating new connections between different molecular events that occur in a single cell. More importantly, the dual-parameter imaging approach described in this study is highly extendable.

1. Introduction

Intracellular molecular events are organized in a complicated network that governs how a cell responds to environmental change. Fluorescent protein (FP)-based biosensors are a powerful tool for revealing molecular events in living cells (DiPilato and Zhang, 2010; Wang et al., 2008). Most FP biosensors utilize green fluorescent protein (GFP)-like superfamily (Ibraheem and Campbell, 2010). Since the first application of GFP for bio-labeling, FPs with different colors have been discovered, making multi-color fluorescence imaging in living cells possible (Chudakov et al., 2010). However, the simultaneous imaging of molecular events in a single living cell with multiple pairs of FP biosensors (multi-parameter imaging) is still in its infancy (Carlson and Campbell, 2009) and is far from being a regular tool for elucidating complex signal networks. The major obstacle in implementing multi-parameter fluorescence imaging experiments is that the spectrum of GFP-like FPs is confined to the narrow visible wavelength (~400–650 nm). Moreover, the excitation and emission spectra of FP are broad and usually cover a range of approximately 100 nm. These intrinsic limitations cause spectral crosstalk between different biosensors, resulting in distorted imaging data.

FP-based biosensors can be divided into two types: fluorescence resonance energy transfer (FRET)-based biosensors, which are composed of genetically fused fluorescent proteins of differing hues, and single fluorescent protein based biosensors. FRET is the non-radiative transfer of energy from a fluorophore in an excited state (the donor) to another fluorophore (the acceptor) that occurs when the distance between the two fluorophores is in the range of 1–10 nm (Jares-Erijman and Jovin, 2003). Currently, most FRET-based biosensors utilize cyan fluorescent protein (CFP)/yellow fluorescent protein (YFP) as the FRET donor/acceptor, while all currently used single-FP biosensors are based on GFP or one of its variants (VanEngelenburg and Palmer, 2008). Given the

* Corresponding author at: Britton Chance Center for Biomedical Photonics, Wuhan National Laboratory for Optoelectronics-Huazhong University of Science and Technology, Wuhan 430074, PR China. Tel.: +86 27 87792033; fax: +86 27 87792034.
E-mail address: czyzzh@mail.hust.edu.cn (Z. Zhang).

0956-5663/$ – see front matter © 2011 Elsevier B.V. All rights reserved.
doi:10.1016/j.bios.2011.10.034

promising prospects of multi-parameter imaging in cell biology, researchers have invested much effort in developing an FP-based biosensor system for multi-parameter imaging that does not suffer from the aforementioned limitations. Ai et al. developed two FRET-based caspase-3 biosensors based on the FRET pairs mTFP1/YFP and mAmetrine/tdTomato (Ai et al., 2008). Although there was some crosstalk between the two biosensors, the delay between the onset of cytoplasmic and nuclear caspase-3 activities was successfully determined during apoptosis. In another report, Piljic and Schultz successfully imaged a single cell with a four-parameter imaging system (Piljic and Schultz, 2008). This landmark study used a CFP/YFP-based FRET biosensor with an orange (mOrange)/red (mCherry)-based biosensor as well as the spatial separation of spectrally identical biosensors. There have been several other successful attempts at multi-parameter imaging, either with FRET-based biosensors using fluorescence lifetime imaging (FLIM) (Grant et al., 2008) or combining FRET-based biosensors with synthetic indicators (Tay et al., 2007).

Although there are several multi-parameter imaging strategies in the literature, the use of single FP-based biosensors has not yet been reported, most likely because of the spectral crosstalk that is involved in pairing single FP-based biosensors with the commonly used CFP/YFP-based FRET biosensors. In this study, we introduce a new FRET pair, based on mVenus (the donor), a variant of yellow fluorescent protein (Nagai et al., 2002) and mKOκ (the acceptor), an orange fluorescent protein (Tsutsui et al., 2008). We demonstrate that the mVenus/mKOκ (abbreviated as YO) FRET pair is spectrally compatible with a single FP biosensor for dual-parameter ratiometric imaging. To demonstrate the ability of this technique to reveal new correlations between two molecular events, we genetically engineered Src kinase and calcium biosensors based on the YO FRET pair, named the YO-Src biosensor and the YO-TnC biosensor, respectively. The existing biosensor Grx1-roGFP2 (Dooley et al., 2004; Gutscher et al., 2008), which specifically measures intracellular GSH/GSSG redox potential (GSH is the reduced form of glutathione and GSSG is the oxidized form of glutathione), was used as a representative single-FP biosensor. By using both YO-Src/YO-Ca^{2+} and Grx1-roGFP2 biosensors, simultaneous imaging of Src/Ca^{2+} signaling and GSH redox potential in a single cell is successfully achieved.

2. Materials and methods

2.1. Plasmid construction

Plasmids encoding biosensors were genetically engineered. For details, please see the methods section of the supporting information.

2.2. Ratiometric imaging

Ratiometric fluorescent imaging was performed with confocal laser-scanning microscope FV1000 (Olympus, Japan) controlled by Fluoview software (Version 1.5) (Olympus, Japan). Immediately before imaging, the DMEM was replaced with a CO_2-independent medium to maintain cells at physiological pH (7.3). For the YO-Src and YO-TnC biosensors, mVenus was excited with a 514 nm laser and emissions of mVenus and mKOκ were collected at 524–540 nm and 560–620 nm, respectively. For the OR-Src and OR-TnC biosensors, mKOκ was excited at 514 nm and emissions of mKOκ and mLumin were collected at 540–560 nm and 600–660 nm, respectively. Because the Grx1-roGFP2 biosensor is ratiometric by excitation (Dooley et al., 2004; Gutscher et al., 2008), two excitation laser lines were used: 405 nm excitation with emission collection from 496 to 560 nm; 488 nm excitation with emission collection from 496 to 515 nm. In the dual ratiometric imaging experiment with the Grx1-roGFP2 and YO-based biosensors, the "time-control" function in the Fluoview software was used to quickly switch between the imaging conditions of each biosensor. Under our imaging conditions, there was a delay of approximately 3 s between imaging of the two biosensors.

2.3. Image processing

Confocal images were processed using *ImageJ* software (http://rsbweb.nih.gov/ij/). For details of the image processing procedure, please see the methods section of the supporting information.

3. Results

3.1. A new FRET pair based on mVenus (donor) and mKOκ (acceptor)

Because all current single-FP biosensors have an emission spectrum analogous to that of GFP (emission peak approximately at 515 nm) (VanEngelenburg and Palmer, 2008), the choice of compatible FRET pairs is limited to FPs that are red-shifted compared with GFP (Wu et al., 2011). Considering this intrinsic limitation and the performance of current available FPs (Wu et al., 2011), we hypothesized that the mVenus/mKOκ (Fig. 1A) and mKOκ/mLumin (Fig. 1B) FRET pairs were potential candidates for pairing to single-FP biosensors in a dual-parameter imaging experiment. mVenus (Nagai et al., 2002), mKOκ (Tsutsui et al., 2008), and mLumin (Chu et al., 2009) perform excellently among yellow FPs (YFPs), orange FPs (OFPs) and red FPs (RFPs), respectively, with fast maturation and high brightness. To test which FRET pair is more appropriate as a biosensor, we genetically constructed Src kinase and calcium biosensors based on the mVenus/mKOκ and mKOκ/mLumin FRET pairs, named YO-Src, YO-TnC, OR-Src and OR-TnC, respectively. The response elements of our Src and Ca^{2+} biosensors are identical to those of previously reported CFP/YFP- based Src biosensor (the response element consists of a SH2 domain and a Src substrate peptide from p130cas) (Wang et al., 2005) and Ca^{2+} biosensor (with a TnC response element) (Mank et al., 2008) (Fig. 1C). The ratio change (ΔR is shown in the form of mean ± SEM) of the YO-Src biosensor (or OR-Src) is the difference in the mVenus/mKOκ (or mKOκ/mLumin) emission ratios before and after the stimulus (e.g., EGF). The ratio change (ΔR) of the YO-TnC biosensor (or OR-TnC) is the difference in the mKOκ/mVenus (or mLumin/mKOκ) emission ratios before and after the stimulus (e.g., ionomycin). We observed that the OR-Src biosensor did not respond to EGF stimulation, whereas the YO-Src biosensor gave a FRET response (ΔR: 34.9% ± 0.7%, $n = 7$; Fig. 1D). For the Ca^{2+} biosensors, YO-TnC (ΔR: 70.8% ± 1.8%, $n = 9$) was also superior to OR-TnC in response to ionomycin (ΔR: 25.0% ± 3.7%, $n = 9$; Fig. 1E). The inappropriateness of the OR FRET pair for use as a biosensor is most likely due to the relatively low brightness of mLumin, resulting in a weakly sensitized emission (Carlson and Campbell, 2009). These results indicate that the YO FRET pair can be used as a biosensor. We therefore used the YO-based biosensor in a dual-parameter imaging experiment with the single FP-based biosensor Grx1-roGFP2.

A previous report has shown that circular permutation mutants of mVenus (cpmVenus) substantially expand the dynamic range of the YC-based Ca^{2+} biosensor (Nagai et al., 2004). To enhance the response of the YO-based biosensor, we replaced the original donor mVenus with its circular permutation mutants. Two circular permutation mutants of mVenus, cpmVenus157 and cpmVenus173, were used as a donor for mKOκ. As shown in Fig. S1B (in the supporting information), cpmVenus173 is superior to mVenus as a

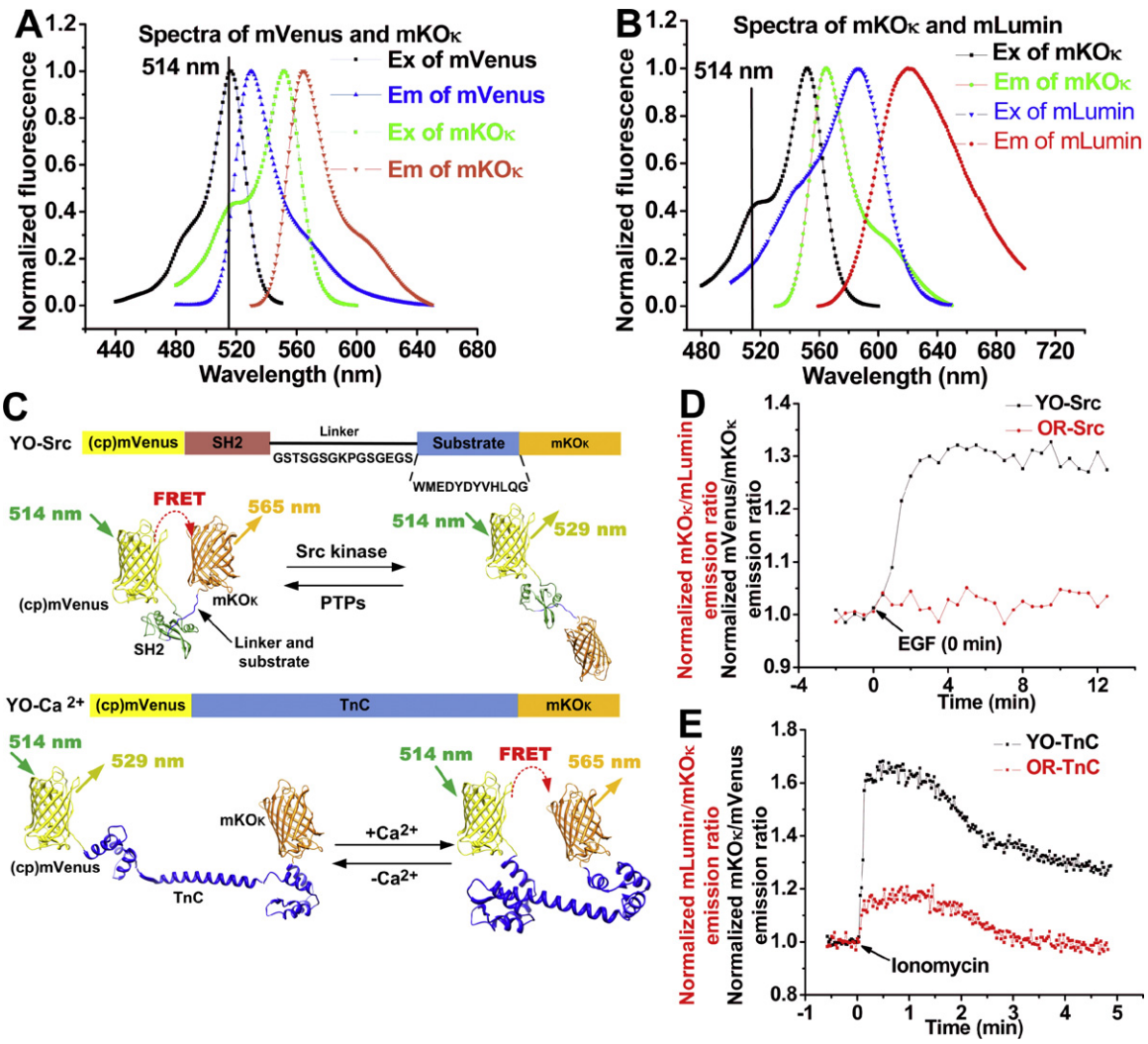

Fig. 1. mVenus and mKOκ are a suitable FRET pair as a biosensor. (A) Excitation and emission spectrum of mVenus and mKOκ. (B) Excitation and emission spectrum of mKOκ and mLumin. Ex: Excitation spectrum; Em: emission spectrum; 514 nm is a commonly used laser line. (C) The structural schematic of YO-Src and YO-TnC biosensors. (D) Emission ratio time courses of the YO-Src (black curve) and OR-Src (red curve) biosensors in response to 100 ng/ml EGF in a HeLa cell. (E) Emission ratio time courses of the YO-TnC (black curve) and OR-TnC (red curve) biosensors in response to 5 μM ionomycin in a HeLa cell. (For interpretation of the references to color in this figure legend, the reader is referred to the web version of the article.)

donor for mKOκ in the Ca^{2+} biosensor (ΔR of cpmVenus173-TnC-mKOκ: 81.9% ± 1.1%, $n = 7$). However, these two mutants in the YO-Src biosensor did not result in an enhanced response (Fig. S1). In the following experiment, the cpmVenus157-Src-mKOκ (named YO-Src1.0) and cpmVenus173-TnC-mKOκ (named YO-TnC1.0) were used to pair with the single FP biosensor Grx1-roGFP2. As shown in Fig. S2, both YO-Src1.0 and YO-TnC1.0 are reversible in living cells. The emission spectrum of the YO-Src 1.0 (or YO-TnC 1.0) biosensor in a HeLa cell before and after EGF (or ionomycin) treatment is shown in Fig. S1C (or Fig. S1D).

3.2. *The mVenus-mKOκ-based biosensor is compatible with the single FP biosensor Grx1-roGFP2 in a dual ratiometric imaging experiment*

After an in-depth analysis of the mVenus, mKOκ, and Grx1-roGFP2 spectra (Fig. 2A and B), we speculated that the main obstacle for dual ratiometric imaging of a YO-based FRET biosensor and Grx1-roGFP2 is the spectra bleeding between mVenus and roGFP2. Excitation of roGFP2 with 488 nm laser line (Fig. 2A) will inevitably excite mVenus, resulting in emission bleeding of mVenus into the roGFP2 channel (Fig. 2B). Furthermore, excitation of mVenus with 514 nm laser line (Fig. 2A) will excite roGFP2, leading to emission bleeding of roGFP2 into the mVenus channel (Fig. 2B). Details on the imaging parameter settings can be found in Fig. 2A and B (or refer to the Section 2). In Grx1-roGFP2 expressed HeLa cells, approximately 1.4% (mean ± SEM: 1.4 ± 0.05%, $n = 37$) of the roGFP2 signal contributes to the mVenus channel (upper panel in Fig. 2C). In mVenus expressed HeLa cells, approximately 5.2% (mean ± SEM: 5.2 ± 0.12%, $n = 34$) of the mVenus signal contributes to the roGFP2 channel (low panel in Fig. 2C).

To test whether the aforementioned degree of cross-talk interferes with dual imaging of the Grx1-roGFP2 and YO-based biosensors in single living cells, the Grx1-roGFP2 and YO-Src 1.0 biosensors were co-transfected into HeLa cells. As indicated in Fig. 2D, upon 100 μM H_2O_2 exposure, the 405/488 nm excitation ratio of Grx1-roGFP2 elevated rapidly and then declined to basal levels while the mVenus/mKOκ emission ratio of the YO-Src 1.0 biosensor remained stable. Similarly, 100 ng/ml EGF caused an increase in the mVenus/mKOκ emission ratio of the YO-Src 1.0 biosensor, whereas the 405/488 nm excitation ratio of Grx1-roGFP2 remained stable (Fig. 2E). Those results demonstrate that the crosstalk between mVenus and roGFP2 causes negligible

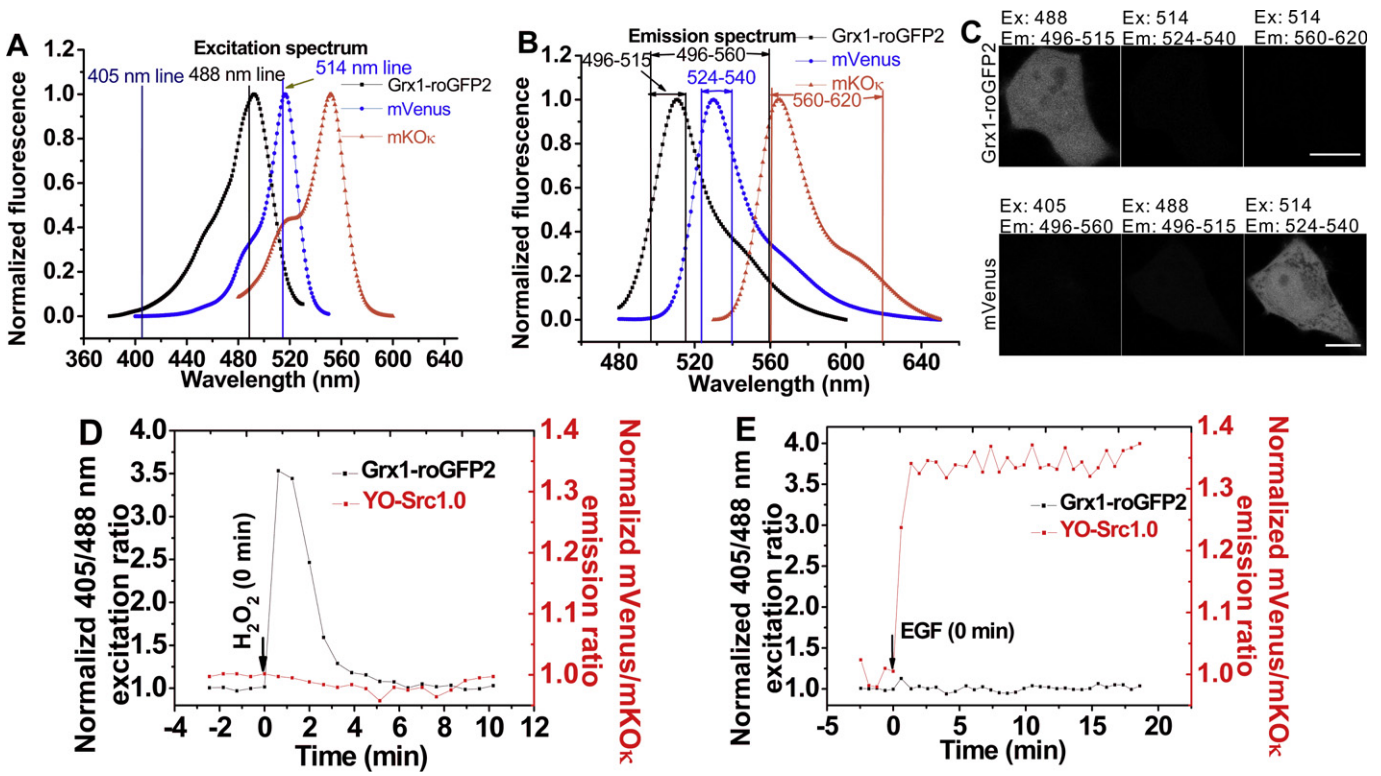

Fig. 2. Feasibility studies on combining mVenus-mKOκ (YO)-based FRET biosensors with the single FP biosensor Grx1-roGFP2 in dual parameter ratiometric imaging. (A) Excitation spectrum of Grx1-roGFP2 (black curve), mVenus (blue curve) (For interpretation of the references to color in this figure legend, the reader is referred to the web version of the article.) and mKOκ (orange curve). The straight lines indicate the excitation laser lines used. Note that Grx1-roGFP2 is in the reduced condition (10 mM DTT). (B) Emission spectrum of Grx1-roGFP2 (black curve), mVenus (blue curve), and mKOκ (orange curve). Acquisition wavelength for each FP is indicated (For details, please refer to Section 2). (C) Cross-excitation between Grx1-roGFP2 and mVenus. The acquisition parameter used to collect mVenus and mKOκ gives some excitation of Grx1-roGFP2 (upper panel). The acquisition parameter used to collect Grx1-roGFP2 gives some excitation of mVenus (low panel). Representative images are shown. Scale bar, 10 μm. (D, E) Control experiments confirm that the ratio change of the Grx1-roGFP2 biosensor does not affect the YO-Src1.0 biosensor, and the ratio change of the YO-Src1.0 biosensor does not affect the Grx1-roGFP2 biosensor. The 100 μM H_2O_2 led to a change in the 405/488 nm excitation ratio for Grx1-roGFP2 without affecting the emission ratio of the YO-Src1.0 biosensor (D), and 100 ng/ml EGF resulted in an emission ratio change of the YO-Src1.0 biosensor without affecting the 405/488 nm excitation ratio of Grx1-roGFP2 (E).

distortion of the ratiometric signal of the YO FRET biosensor and Grx1-roGFP2, and intensity correction is not required. Notably, two recently developed dual-parameter imaging approaches that make use of the two FRET pairs do require further image correction because of the relatively high cross-talk between two biosensors (Ai et al., 2008; Nagai et al., 2009).

Based on these results, we conclude that the Grx1-roGFP2 and YO-based biosensors are spectrally compatible for dual imaging applications.

3.3. Simultaneous monitoring of the kinetics of GSH-redox potential and Src signaling using the Grx1-roGFP2 and YO-Src 1.0 biosensors in living cells

EGF-induced endogenous H_2O_2 is considered a positive regulator in facilitating propagation of protein tyrosine kinase (such as Src kinase)-mediated tyrosine phosphorylation signaling (Lee et al., 1998). H_2O_2 inhibits the activity of protein tyrosine phosphatases (PTPs) by oxidizing a cysteine in the active site of PTPs to create a cysteine–sulfenic derivative (Chiarugi and Buricchi, 2007; Chiarugi et al., 2001). A direct consequence of elevated cellular H_2O_2 levels is a disturbance of the GSH-based redox system whose indicator is GSH redox potential (Jones, 2002). However, the kinetic correlation between tyrosine phosphorylation signaling and GSH redox potential under H_2O_2 exposure is not yet well understood. To demonstrate the capability of our dual-parameter imaging technique in revealing new insights into two molecular events, we set out to study the kinetic relationship of EGF-induced Src signaling and GSH redox potential under H_2O_2 treatment by co-transfecting YO-Src 1.0 and Grx1-roGFP2 biosensors into HeLa cells.

We first examined the response of the Grx1-roGFP2 and YO-Src 1.0 biosensors upon EGF stimulation alone. Fig. 3A shows that after the addition of 25 ng/ml EGF, the mVenus/mKOκ emission ratio of the YO-Src 1.0 biosensor rapidly elevated and maintained a constant level over the course of the imaging session, whereas the 405/488 nm excitation ratio of Grx1-roGFP2 did not change. This result is consistent with the previous reports that show that EGF does not produce a global alteration of the GSH redox system (Halvey et al., 2005). Next, we treated HeLa cells with exogenous H_2O_2 after stimulation by EGF. As shown in Fig. 3B and C, the addition of 1 mM H_2O_2 caused a rapid increase in the 405/488 nm excitation ratio of Grx1-roGFP2, indicating the conversion of cellular GSH to GSSG. Following this rapid increase, the 405/488 excitation ratio gradually declined, indicating the recovery of GSSG to GSH and regaining the balance of the GSH redox system. Interestingly, the decline in the 405/488 nm excitation ratio of Grx1-roGFP2 is accompanied by a slow decrease in the mVenus/mKOκ emission ratio of YO-Src 1.0. This temporal correlation of the GSH redox potential and Src signaling strongly suggests that Src signaling is regulated by the GSH redox system. Because the mVenus/mKOκ emission ratio of the YO-Src 1.0 biosensor intrinsically reflects the relative activity of Src kinase and protein tyrosine phosphatases (PTPs), the decrease in the mVenus/mKOκ emission ratio induced by H_2O_2 suggests that the formerly inhibited activity of cellular PTPs might be recovered (Lee et al., 1998). To test this hypothesis, we pretreated HeLa cells with 500 μM vanadate, which

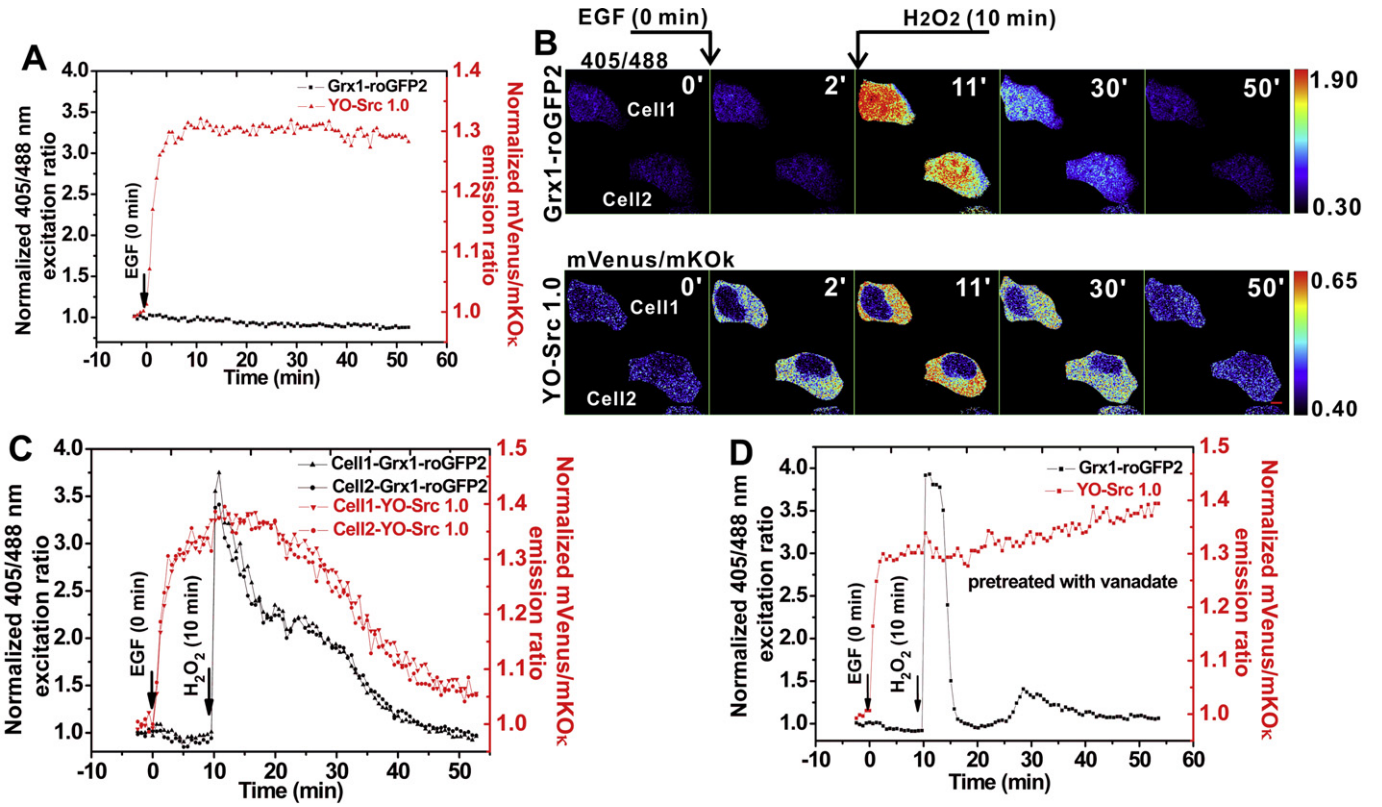

Fig. 3. Simultaneous imaging of the kinetics of Src signaling and GSH redox potential using the YO-Src1.0 and Grx1-roGFP biosensors. (A) Emission ratio (red curve) (For interpretation of the references to color in this figure legend, the reader is referred to the web version of the article.) time courses of the YO-Src1.0 biosensor and 405/488 excitation ratio (black curve) time courses of Grx1-roGFP2 in response to 25 ng/ml EGF in a HeLa cell. (B) Pseudocolored ratio images of HeLa cells expressing dual biosensors at the indicated times (in minutes). At 0 min, 25 ng/ml EGF was added, and 1 mM H_2O_2 was added at 10 min. (C) Emission ratio (red curve) time courses of the YO-Src1.0 biosensor and 405/488 excitation ratio (black curve) time courses of Grx1-roGFP2 in (B). A region in the cytoplasm was selected for calculating ratios. (D) The ratio time course of the YO-Src1.0 and Grx1-roGFP2 biosensors in a HeLa cell pre-treated with 500 μM vanadate, a specific PTP inhibitor, for 15 min. At 0 min, 25 ng/ml EGF was added, and 1 mM H_2O_2 was added at 10 min. The results are representative of three independent experiments. Scale bar, 10 μm.

specifically inhibits the activity of PTPs. As indicated in Fig. 3D, the mVenus/mKOκ emission ratio of the YO-Src 1.0 biosensor did not decrease after an initial increase, verifying our hypothesis that the exogenous H_2O_2-induced decrease in Src signaling in Fig. 3C can be ascribed to the recovered activity of PTPs. This evidence also suggests that the negative regulation of Src signaling by the GSH redox system is mediated by its effect on recovering the activity of PTPs.

In summary, our dual parameter imaging experiments established a negative role of H_2O_2 in regulating EGF-induced Src signaling. H_2O_2 is not always a positive regulator. When exogenously added, H_2O_2 can instead attenuate tyrosine phosphorylation signaling by its effect on the GSH redox system.

3.4. Simultaneous monitoring of the kinetics of GSH-redox potential and Ca^{2+} signaling using the Grx1-roGFP2 and YO-TnC1.0 biosensors in living cells

In addition to inducing an imbalance of the GSH redox potential, evidence has shown that exogenous H_2O_2 can also elicit an elevation in intracellular calcium (Suzuki et al., 1998). However, there are no reports showing the kinetics of GSH-redox potential and Ca^{2+} signaling upon H_2O_2 treatment in an individual cell. Toward this end, HeLa cells were co-transfected with plasmids encoding YO-TnC 1.0 and Grx1-roGFP2 biosensors. Fig. 4A and B show the kinetics of the Ca^{2+} signaling and GSH-redox potential in HeLa cells in response to 5 mM H_2O_2. Interestingly, the cells displayed two distinct types of Ca^{2+} signaling, suggesting that there is heterogeneity among cells. This experiment again demonstrates the ability of our dual-parameter imaging approach to investigate previously inaccessible dual molecular kinetics in a single cell.

4. Discussion

We have developed a novel combination of biosensors for dual-parameter ratiometric imaging consisting of an mVenus/mKOκ FRET biosensor and a single FP-based biosensor. In addition to providing two combinations of biosensors (YO-Src/Ca^{2+} and Grx1-roGFP2) for dual-parameter ratiometric imaging, our approach is highly extendable. Currently used biosensors are mainly CFP/YFP-based FRET biosensors and single GFP-based biosensors. We suggest that CFP/YFP-based FRET biosensors can be converted into mVenus/mKOκ-based biosensors and that the Grx1-roGFP2 can be replaced by other single GFP-based biosensors. Through these combinations, toolkits for dual-parameter ratiometric imaging will be extensively expanded.

The dual-parameter ratiometric imaging approach reported here benefits from the introduction of a new mVenus/mKOκ FRET pair whose ratiometric signal can be distinguished easily from that of existing single FP-based biosensors without further correction. Compared with the popular CFP/YFP FRET pair, the Förster radius of the mVenus/mKOκ pair is significantly higher (6.10 nm for mVenus/mKOκ pair vs. 5.0 nm for CFP/YFP pair) (Kremers et al., 2006). Notably, there is some spectral cross-talk between mVenus and mKOκ; mKOκ can be partially excited when exciting mVenus (Fig. 1A), and the mVenus fluorescence can bleed-through into the mKOκ channel (Fig. S3). Although these two types of crosstalk can be corrected with standard three-channel imaging methods, such

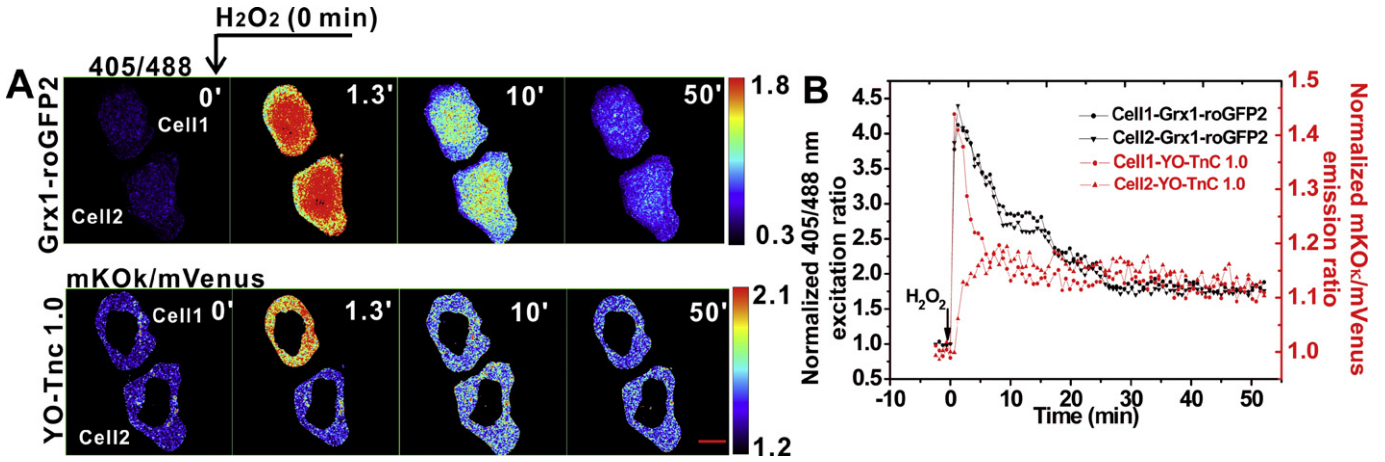

Fig. 4. Simultaneous imaging of the kinetics of Ca^{2+} signaling and GSH redox potential using the YO-TnC1.0 and Grx1-roGFP biosensors. (A) Pseudocolored ratio images of HeLa cells expressing dual biosensors (Grx1-roGFP2 and YO-TnC1.0 biosensors) at the indicated times. At 0 min, 5 mM H_2O_2 was added. (B) Emission ratio (red curve) (For interpretation of the references to color in this figure legend, the reader is referred to the web version of the article.) time courses of the YO-TnC1.0 biosensor and 405/488 excitation ratio (black curve) time courses of Grx1-roGFP2 in (B). The results are representative of three independent experiments. Scale bar, 10 μm.

crosstalk is unfavorable for obtaining a large dynamic range in ratiometric imaging (Vogel et al., 2006). Despite those limitations, the dynamic range of the YO-Src1.0 biosensor (35%) is comparable to that of the original Src biosensor based on the ECFP/mCitrine pair (25–35%) (Wang et al., 2005). Nevertheless, for the Ca^{2+} biosensor, the dynamic range of the YO pair is inferior to that of the CFP/YFP pair (82% vs. 400%) (McCombs and Palmer, 2008). It should be noted that the CFP/YFP based Ca^{2+} biosensor is extensively optimized in linker lengths (Mank et al., 2008; Miyawaki et al., 1997) and the choice of the rational circular permuted YFP variant (cpYFP) (Nagai et al., 2004). In the future, the YO-based FRET biosensor can also undergo similar optimizations to improve its dynamic range.

By dual-parameter imaging of Src signaling and GSH redox potential, we demonstrated a new role of H_2O_2 in negatively regulating Src-mediated tyrosine phosphorylation signaling (Fig. 3C), which seems to contradict with the orthodox view. The prevailing view asserts that H_2O_2 plays a positive role in modulating tyrosine phosphorylation signaling by inhibiting PTPs' activity (Chiarugi and Buricchi, 2007). We speculate that this discrepancy might arise because the exogenously added H_2O_2 under our conditions could disturb the global redox balance, resulting in oxidative stress (Jones, 2002). To counteract H_2O_2-induced oxidative stress, the anti-oxidant defense system is triggered by activating a series of relevant enzymes such as the H_2O_2-degrading enzyme Gpx1 (Ng et al., 2007). These activated enzymes clear excessive H_2O_2, which restores the redox balance. This recovery is reflected in our results by the gradual decline of the 405/488 nm excitation ratio of Grx1-roGFP2 (Fig. 3C). During this recovery process, the PTPs' enzymatic activity is rescued by GSH-dependent reduction of previously oxidized cysteines (Chiarugi et al., 2001), leading to the attenuation of Src signaling (Fig. 3C and D). Our dual-parameter ratiometric imaging approach demonstrated that H_2O_2 is not always a positive regulator of tyrosine phosphorylation signaling as previously hypothesized. In the case of global oxidative stress, H_2O_2 can instead attenuate tyrosine phosphorylation signaling.

5. Conclusion

In summary, we have successfully established a novel dual-parameter ratiometric imaging approach based on the mVenus/mKOκ-based FRET biosensor and a single FP-based biosensor. By using this approach, we achieved simultaneous imaging of Src/Ca^{2+} signaling and the GSH redox potential in a single cell with a spatiotemporal precision that was previously inaccessible. Because the existing CFP/YFP-based FRET biosensors can be converted into an mVenus/mKOκ-based biosensor and Grx1-roGFP2 can be substituted with other single FP biosensors, we believe that the dual-parameter ratiometric imaging approach described in this study can be extensively applied for the identification and elucidation of the interplay and relative kinetics of two molecular events in single living cells.

Acknowledgements

We thank Dr. Atsushi Miyawaki for providing mVenus and mKO, Dr. Tobias P Dick for Grx1-roGFP2 and Dr. Oliver Griesbeck for TN-XXL. The authors also thank the Analytical and Testing Center of Huazhong University of Science and Technology for spectral measurements. This work was supported by National Major Scientific Research Program of China (Grant No. 2011CB910401), National Natural Science Foundation of China (Grant No. 81172153, 30911120489, 30800339, 30800208), Program for New Century Excellent Talents in University of China (NCET-08-0220 to Z.H. Zhang).

Appendix A. Supplementary data

Supplementary data associated with this article can be found, in the online version, at doi:10.1016/j.bios.2011.10.034.

References

Ai, H.W., Hazelwood, K.L., Davidson, M.W., Campbell, R.E., 2008. Nat. Methods 5 (5), 401–403.
Carlson, H.J., Campbell, R.E., 2009. Curr. Opin. Biotechnol. 20 (1), 19–27.
Chiarugi, P., Buricchi, F., 2007. Antioxid. Redox Signal. 9 (1), 1–24.
Chiarugi, P., Fiaschi, T., Taddei, M.L., Talini, D., Giannoni, E., Raugei, G., Ramponi, G., 2001. J. Biol. Chem. 276 (36), 33478–33487.
Chu, J., Zhang, Z.H., Zheng, Y., Yang, J., Qin, L.S., Lu, J.L., Huang, Z.L., Zeng, S.Q., Luo, Q.M., 2009. Biosens. Bioelectron. 25 (1), 234–239.
Chudakov, D.M., Matz, M.V., Lukyanov, S., Lukyanov, K.A., 2010. Physiol. Rev. 90 (3), 1103–1163.
DiPilato, L.M., Zhang, J., 2010. Curr. Opin. Chem. Biol. 14 (1), 37–42.
Dooley, C.T., Dore, T.M., Hanson, G.T., Jackson, W.C., Remington, S.J., Tsien, R.Y., 2004. J. Biol. Chem. 279 (21), 22284–22293.
Grant, D.M., Zhang, W., McGhee, E.J., Bunney, T.D., Talbot, C.B., Kumar, S., Munro, I., Dunsby, C., Neil, M.A.A., Katan, M., French, P.M.W., 2008. Biophys. J. 95 (10), L69–L71.
Gutscher, M., Pauleau, A.L., Marty, L., Brach, T., Wabnitz, G.H., Samstag, Y., Meyer, A.J., Dick, T.P., 2008. Nat. Methods 5 (6), 553–559.
Halvey, P.J., Watson, W.H., Hansen, J.M., Go, Y.M., Samali, A., Jones, D.P., 2005. Biochem. J. 386, 215–219.
Ibraheem, A., Campbell, R.E., 2010. Curr. Opin. Chem. Biol. 14 (1), 30–36.

Jares-Erijman, E.A., Jovin, T.M., 2003. Nat. Biotechnol. 21 (11), 1387–1395.
Jones, D.P., 2002. Method Enzymol. 348, 93–112.
Kremers, G.J., Goedhart, J., van Munster, E.B., Gadella, T.W.J., 2006. Biochemistry-U.S. 45 (21), 6570–6580.
Lee, S.R., Kwon, K.S., Kim, S.R., Rhee, S.G., 1998. J. Biol. Chem. 273 (25), 15366–15372.
Mank, M., Santos, A.F., Direnberger, S., Mrsic-Flogel, T.D., Hofer, S.B., Stein, V., Hendel, T., Reiff, D.F., Levelt, C., Borst, A., Bonhoeffer, T., Hubener, M., Griesbeck, O., 2008. Nat. Methods 5 (9), 805–811.
McCombs, J.E., Palmer, A.E., 2008. Methods 46 (3), 152–159.
Miyawaki, A., Llopis, J., Heim, R., McCaffery, J.M., Adams, J.A., Ikura, M., Tsien, R.Y., 1997. Nature 388 (6645), 882–887.
Nagai, T., Ibata, K., Park, E.S., Kubota, M., Mikoshiba, K., Miyawaki, A., 2002. Nat. Biotechnol. 20 (1), 87–90.
Nagai, T., Tomosugi, W., Matsuda, T., Tani, T., Nemoto, T., Kotera, I., Saito, K., Horikawa, K., 2009. Nat. Methods 6 (5), 351–353.
Nagai, T., Yamada, S., Tominaga, T., Ichikawa, M., Miyawaki, A., 2004. Proc. Natl. Acad. Sci. U.S.A. 101 (29), 10554–10559.
Ng, C.F., Schafer, F.Q., Buettner, G.R., Rodgers, V.G.J., 2007. Free Radic. Res. 41 (11), 1201–1211.
Piljic, A., Schultz, C., 2008. ACS Chem. Biol. 3 (3), 156–160.
Suzuki, Y.J., Cleemann, L., Abernethy, D.R., Morad, M., 1998. Free Radic. Biol. Med. 24 (2), 318–325.
Tay, L.H., Griesbeck, O., Yue, D.T., 2007. Biophys. J. 93 (11), 4031–4040.
Tsutsui, H., Karasawa, S., Okamura, Y., Miyawaki, A., 2008. Nat. Methods 5 (8), 683–685.
VanEngelenburg, S.B., Palmer, A.E., 2008. Curr. Opin. Chem. Biol. 12 (1), 60–65.
Vogel, S.S., Thaler, C., Koushik, S.V., 2006. Sci. STKE 331, re2.
Wang, Y.X., Botvinick, E.L., Zhao, Y.H., Berns, M.W., Usami, S., Tsien, R.Y., Chien, S., 2005. Nature 434 (7036), 1040–1045.
Wang, X.P., Chen, T.S., Wang, L.X., Sun, L., 2008. J. Innovative Opt. Health Sci. 1 (1), 151–156.
Wu, B., Piatkevich, K.D., Lionnet, T., Singer, R.H., Verkhusha, V.V., 2011. Curr. Opin. Cell Biol. 23 (3), 310–317.